nature geoscience

ARTICLES

PUBLISHED ONLINE: 30 JANUARY 2017 | DOI: 10.1038/NGEO2888

Enhanced weathering and CO_2 drawdown caused by latest Eocene strengthening of the Atlantic meridional overturning circulation

Geneviève Elsworth[1*], Eric Galbraith[1,2,3], Galen Halverson[1] and Simon Yang[4]

On timescales significantly greater than 10^5 years, atmospheric p_{CO_2} is controlled by the rate of mantle outgassing relative to the set-point of the silicate weathering feedback. The weathering set-point has been shown to depend on the distribution and characteristics of rocks exposed at the Earth's surface, vegetation types and topography. Here we argue that large-scale climate impacts caused by changes in ocean circulation can also modify the weathering set-point and show evidence suggesting that this played a role in the establishment of the Antarctic ice sheet at the Eocene–Oligocene boundary. In our simulations, tectonic deepening of the Drake Passage causes freshening and stratification of the Southern Ocean, strengthening the Atlantic meridional overturning circulation and consequently raising temperatures and intensifying rainfall over land. These simulated changes are consistent with late Eocene tectonic reconstructions that show Drake Passage deepening, and with sediment records that reveal Southern Ocean stratification, the emergence of North Atlantic Deep Water, and a hemispherically asymmetric temperature change. These factors would have driven intensified silicate weathering and can thereby explain the drawdown of carbon dioxide that has been linked with Antarctic ice sheet growth. We suggest that this mechanism illustrates another way in which ocean–atmosphere climate dynamics can introduce nonlinear threshold behaviour through interaction with the geologic carbon cycle.

The rapid emplacement of a large ice sheet on Antarctica at the Eocene–Oligocene (E–O) boundary (33.7 million years ago (Ma)) is among the most dramatic climate events of the Cenozoic era. Although the timescale for this event is well established, the driving mechanism remains controversial, with two main contrasting hypotheses. The first is based on geologic evidence that the Drake Passage and Tasman Gateway both expanded during the late Eocene and posits that the thermal isolation of Antarctica within a circumpolar Southern Ocean caused local cooling, triggering nucleation of the ice sheet[1]. The second hypothesis states that global cooling, as a result of gradually declining atmospheric p_{CO_2}, allowed an incipient ice sheet to grow rapidly when p_{CO_2} crossed a critical threshold of 700–900 ppm (refs 2,3). Both arguments have observational support: the Drake Passage significantly widened and deepened within a few million years of the E–O boundary[4], and proxy reconstructions show a long-term decline in atmospheric p_{CO_2} and seawater temperatures from the early Eocene climatic optimum[3,5]. Here, we propose a new hypothesis that links these two mechanisms.

Modelled impact of Drake Passage deepening

Simulations with global coupled ocean–atmosphere models have shown that opening the Drake Passage impedes the advection of warm subtropical waters to the Antarctic[6,7], consistent with the thermal isolation hypothesis[1]. However, the deepening of the Drake Passage also has an impact on global deep-water formation. When the Drake Passage is closed or very shallow, Southern Ocean surface waters tend to be considerably denser than those of the North Atlantic, and consequently the global deep ocean is dominantly ventilated from the waters around Antarctica[7], consistent with proxy evidence from the middle Eocene[8]. In contrast, when the Drake Passage is open, the geostrophic transport of shallow, saline waters from the subtropics to high Southern latitudes is restricted, causing the high-latitude Southern Ocean surface to freshen[6,7].

The decrease in density of Southern Ocean surface waters provides an opportunity for North Atlantic waters to assume the role of deep-water generation via the Atlantic meridional overturning circulation (AMOC). Supplementary Fig. 1 shows how the AMOC, simulated by a coupled ocean–atmosphere model (Methods), differs given a Drake Passage depth of 300 m versus 1,500 m, a depth range that could have been rapidly transited in the late Eocene[4]. Concomitant changes in North Atlantic bathymetry, due to subsidence of the Greenland–Scotia Ridge, would be expected to have further promoted the development of an AMOC at this time[9].

Reconstructed changes during the late Eocene

Figure 1 shows a collection of deep-water and temperature proxy records that together corroborate the model-based expectation of a stratification of the Southern Ocean and strengthening of the AMOC in the late Eocene. Benthic foraminiferal $\delta^{13}C$ from two sites in the intermediate (1,500 m palaeodepth) and deep (3,700 m palaeodepth) South Atlantic show very similar $\delta^{13}C$ values prior to 36 Ma. This pattern is consistent with a chemically homogeneous water mass as would be expected if the Southern Ocean had been filled throughout this depth range by waters formed in the circum-Antarctic. However, for the ~1.5 Myr prior to the E–O boundary, a large $\delta^{13}C$ gradient developed between the intermediate and deep sites (Fig. 1a). The lower $\delta^{13}C$ at depth suggests the development

[1]Department of Earth and Planetary Sciences, McGill University, 3450 University Street, Montreal, Quebec H3A 0E8, Canada. [2]Institució Catalana de Recerca i Estudis Avançats (ICREA), 08010 Barcelona, Spain. [3]Institut de Ciencia i Technologia Ambientals (ICTA) and Department of Mathematics, Universitat Autònoma de Barcelona, 08193 Barcelona, Spain. [4]Department of Environmental Systems Science, ETH Zürich, Universitätsstrasse 16, Zürich 8092, Switzerland. *e-mail: genevieve.elsworth@gmail.com

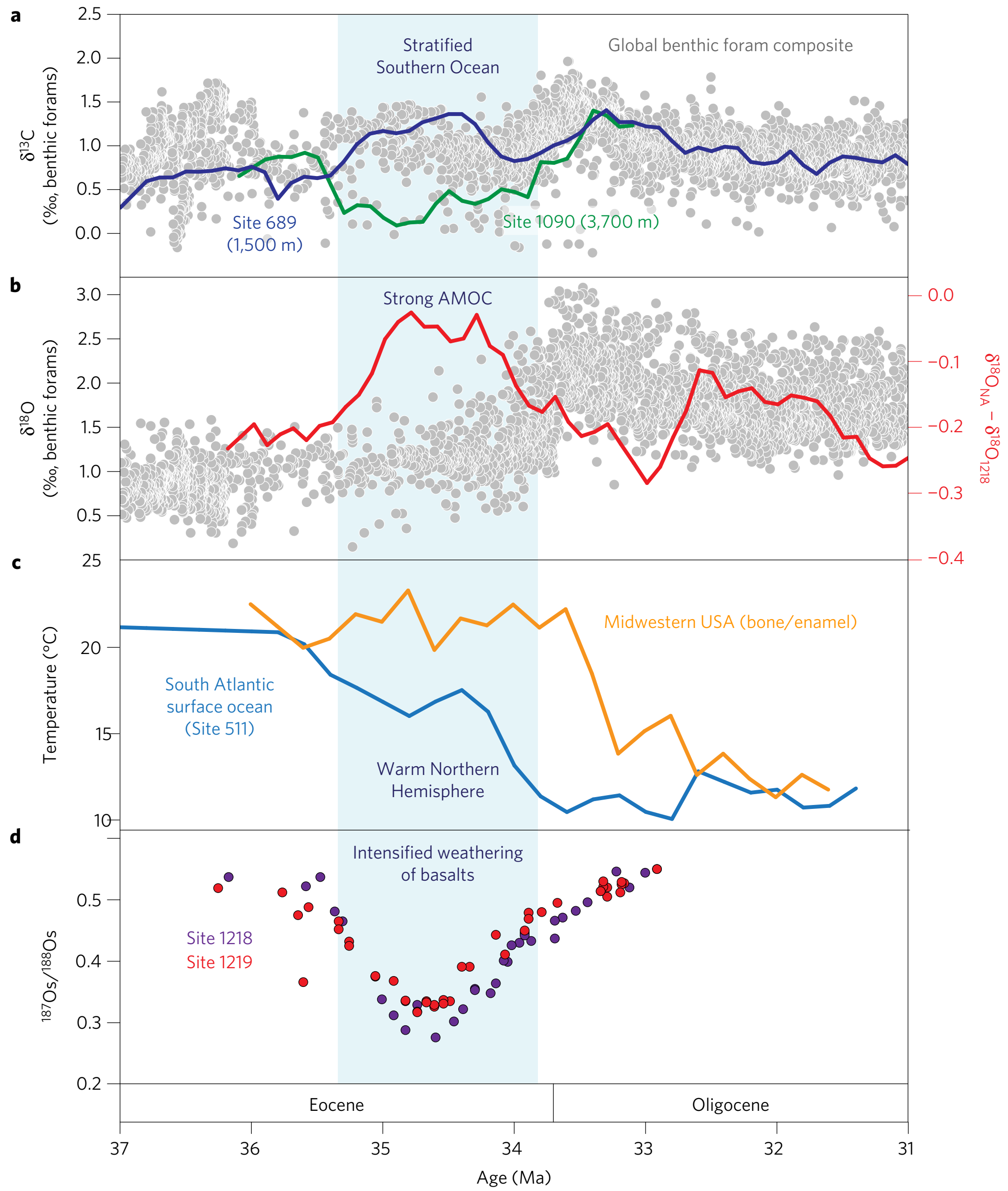

Figure 1 | Proxy records from the late Eocene and early Oligocene. **a**, Southern Ocean (Maud Rise) Site 689 (palaeodepth ~1,500 m) benthic foraminiferal $\delta^{13}C$ data[24] (blue curve) and South Atlantic (Agulhas Ridge) Site 1090 (palaeodepth ~3,700 m) benthic foraminiferal $\delta^{13}C$ data[25] (green curve). $\delta^{13}C$ data sets have been smoothed using local regression interpolation. Background grey dots show benthic foraminiferal $\delta^{13}C$ measurements from a global compilation[26]. **b**, Smoothed deep-water $\delta^{18}O$ gradient between the North Atlantic and the Central Pacific as calculated from interpolated and time-averaged benthic foraminiferal data from the North Atlantic compilation[23] and central Pacific Ocean Drilling Program Site 1218 (palaeodepth ~4,000 m; ref. 27) (red curve). Background grey dots show compiled $\delta^{18}O$ measurements, as in **a**. **c**, Bone and tooth enamel $\delta^{18}O$ data from Midwestern USA mammals[12] (orange curve), and South Atlantic surface ocean temperatures from South Atlantic Site 511 (Falklands Plateau) from the alkenone unsaturation index ($U^{K'}_{37}$; refs 28,29) (blue curve). Both curves were generated by local regression interpolation of all published data. **d**, Osmium isotope ratios measured on bulk sediments from Integrated Ocean Drilling Program Sites 1218 and 1219 in the equatorial Pacific[20].

of waters with a large carbon isotopic disequilibrium and/or a large accumulation of respired carbon, in contrast to the waters above. This strong vertical gradient in $\delta^{13}C$ is similar to the vertical gradient observed during glacial maxima of the Quaternary period[10] and is difficult to explain by any mechanism other than stratification of the Southern Ocean.

Benthic $\delta^{18}O$ records have been previously interpreted to show the development of a distinct North Atlantic Deep Water (NADW) endmember in the late Eocene[8,11]. Figure 1b shows the difference between the $\delta^{18}O$ of the North Atlantic and that of the deep Pacific Ocean (Ocean Drilling Program Site 1218), as a proxy for the contribution of NADW to the global deep ocean. The elimination of the $\delta^{18}O$ gradient between the North Atlantic and deep Pacific in the latest Eocene (~34 to 35 Ma) suggests a strong contribution of NADW to the global deep sea, consistent with the presence of a strong AMOC.

Surface temperature reconstructions are also consistent with the development of a strong AMOC immediately prior to the E–O boundary. As shown in Fig. 1c, the surface ocean over the Falkland Plateau cooled steadily from ~36 Ma to the E–O boundary, whereas terrestrial records from the Midwestern United States indicate sustained warmth until the onset of the Oligocene[12]. Terrestrial records from northwestern Europe similarly indicate sustained warm or slightly increasing temperatures[13] prior to abrupt cooling at the E–O boundary. This reconstructed asymmetry of Northern versus Southern Hemisphere temperature histories would not be expected from CO_2-driven cooling alone, but is entirely consistent with a strengthening AMOC that warmed the Northern Hemisphere at the expense of the Southern Hemisphere. Thus, proxy evidence supports the development of the AMOC in response to tectonic forcing prior to the E–O boundary. However, Southern Ocean stratification and AMOC strengthening occurred more than 1 Myr prior to Antarctic glaciation. This offset suggests that the thermal isolation of Antarctica caused by the widening of Southern Ocean gateways alone was insufficient to drive glaciation[14].

Impact of enhanced AMOC on silicate weathering

We suggest that the missing piece in the triggering of Antarctic glaciation was a drawdown in atmospheric p_{CO_2} resulting from an AMOC-driven increase in the intensity of silicate weathering. Silicate weathering is thought to exert a strong negative feedback on atmospheric p_{CO_2}, via the effect of p_{CO_2} on temperature and precipitation[15,16], thereby determining the atmospheric p_{CO_2} for a given rate of carbon release on any timescale significantly exceeding the $\sim 10^5$ yr residence time of carbon in the ocean–atmosphere system[17]. On such timescales, the silicate weathering feedback supersedes any effects of air–sea partitioning on CO_2, such as the ocean soft-tissue pump or alkalinity-controlled solubility[18]. It has previously been shown that the intensity of silicate weathering for a given global temperature and precipitation pattern depends on topography[19] and distributions of rock types at the Earth's surface[20]. Here we argue that a redistribution of regional temperature and precipitation patterns resulting from a change in ocean circulation can also significantly alter the intensity of silicate weathering.

The strengthening of the AMOC triggered by our simulated Drake Passage deepening results in an increase of global surface air temperature over land by $\sim 1\,^{\circ}C$, despite negligible change in the global average surface temperature, due to the fact that the Northern Hemisphere contains most of the land area (Fig. 2a). More importantly, precipitation increases over land by 5%, largely due to a northward shift of the intertropical convergence zone. The change is especially pronounced in the tropics, with amplifications of annual precipitation by a factor of 20–100% in the North Atlantic, central Americas, North Africa and South Asia (Fig. 2b). Notably, almost all regions that experience high chemical weathering rates at the present day are shown to undergo increased precipitation (Supplementary Fig. 2). The model-based expectation of intensified weathering is also supported by the seawater Os isotope record, which shows a pronounced excursion during the final 1.5 Myr of the Eocene[21] (Fig. 1d). This anomaly is easily explained by enhanced hydrolysis of exposed mafic volcanic rocks, which have low $^{187}Os/^{188}Os$ ratios and are highly prone to chemical weathering[20]. The amplified weathering would have drawn down atmospheric p_{CO_2}, driving global cooling.

Atmospheric p_{CO_2} decline caused by enhanced weathering

We provide a rough estimate of the CO_2 drawdown that would have occurred, in order to bring the carbon cycle back into balance, by comparing the AMOC-driven precipitation change with the simulated precipitation over land that occurs over a range of CO_2 concentrations in the same model (Fig. 3). The model suggests that in order to achieve a 5% decrease in precipitation through the drawdown of CO_2 (required to bring the carbon burial flux back into balance with an invariant carbon outgassing flux), atmospheric p_{CO_2} would need to have been reduced from $\sim$900 to 600 ppmv. This magnitude of change agrees remarkably well with the change required by ice sheet models to nucleate an Antarctic ice sheet[2,14].

This scenario implies that tectonics could have triggered growth of the Antarctic ice sheet at the E–O boundary by deepening the Drake Passage below a critical threshold that stimulated onset of a

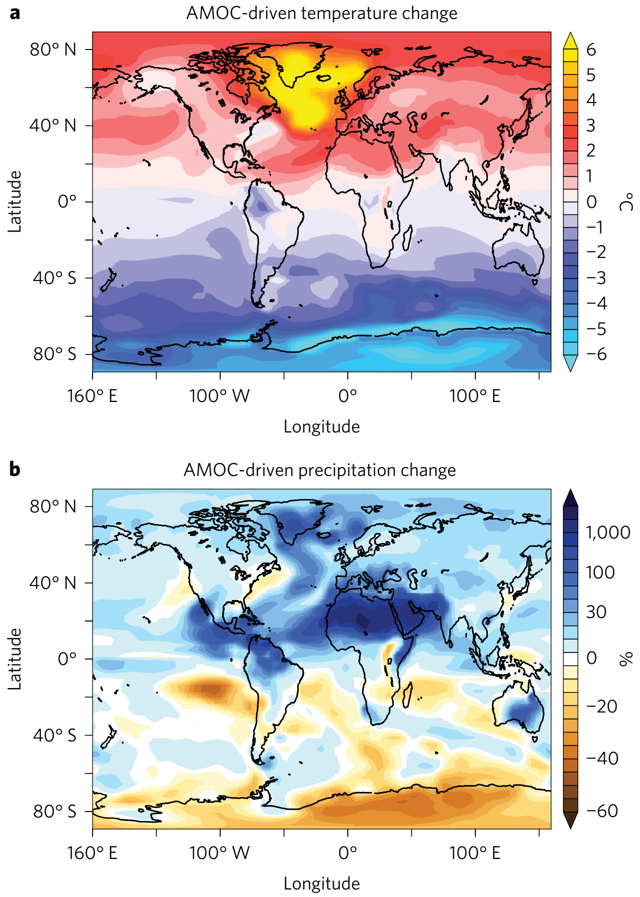

Figure 2 | Simulated impact of Drake Passage deepening on global surface air temperature and precipitation. Each panel shows the difference between an equilibrium simulation with a Drake Passage depth 1,500 m (deep) and one with a Drake Passage depth 300 m (shallow). **a**, Change in surface air temperature (deep–shallow). **b**, Relative change in precipitation (deep/shallow).

strong AMOC. By isolating Antarctica from warm, salty subtropical waters, the deepening of southern gateways cooled the Southern Ocean and primed the continent for glaciation, while allowing the North Atlantic to initiate strong overturning circulation. Acceleration of silicate weathering resulting from onset of the AMOC would have drawn down atmospheric p_{CO_2}, toward a critical threshold to trigger the rapid growth of an Antarctic ice sheet[14].

Finally, we note that the $\delta^{13}C$ and $\delta^{18}O$ data indicate destratification of circum-Antarctic waters and rapid dwindling of the AMOC following the onset of Antarctic glaciation (Fig. 1a,b). These observations are consistent with the modelling results of ref. 22, showing a large increase in deep-water formation in the Southern Ocean once the Antarctic ice sheet had formed. The rejuvenated formation of dense Antarctic Deep Water would have weakened the AMOC, accounting for the abrupt cooling of the North Atlantic at this time and consequent closure of the inter-hemisphere temperature gradient (Fig. 1c). The potentially large effects of ice sheet growth on the air–sea partitioning of carbon[23] could have modulated changes in CO_2 during and immediately following the transition, further lowering CO_2 over a short timescale despite the weakening of silicate weathering that would have arisen from the AMOC collapse. The fact that the Antarctic ice sheet remained stable in the early Oligocene, despite hints of a return to higher CO_2 following the transition[3], could then be consistent with the operation of strong stabilizing feedbacks that helped to maintain the Antarctic ice sheet once established[14].

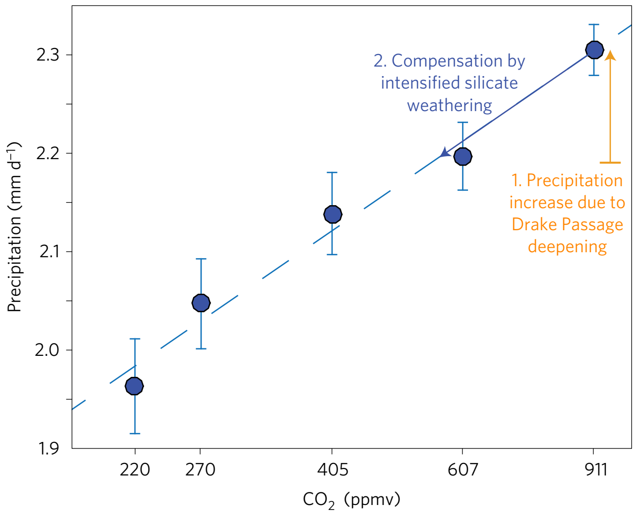

Figure 3 | Simulated impact of Drake Passage deepening and atmospheric CO_2 on precipitation over land. Blue symbols show the globally averaged precipitation over land, averaged over the four orbital configurations for each level of atmospheric p_{CO_2}, whereas the error bars show the 1 s.d. variation among the different orbital configurations. CO_2 concentrations are logarithmically spaced, to reflect the logarithmic dependence of radiative forcing on CO_2. The dashed blue line shows the linear regression ($r^2 = 0.98$). The vertical orange line indicates the simulated change in globally averaged precipitation over land that results from the deepening of Drake Passage from 300 to 1,500 m, as shown in Fig. 2b. For a decrease in atmospheric p_{CO_2} to compensate for the perturbation caused by Drake Passage deepening would require, all else being equal, a reduction of precipitation equivalent to the length of the orange bar, for example, from 900 to 600 ppmv. Note that this simple calculation ignores spatial heterogeneity of rock types and other potentially complicating factors.

Methods

Methods, including statements of data availability and any associated accession codes and references, are available in the online version of this paper.

Received 14 October 2016; accepted 3 January 2017; published online 30 January 2017; corrected online 15 February 2017

References

1. Kennett, J. P. Cenozoic evolution of Antarctic glaciation, the circum-Antarctic Ocean, and their impact on global paleogeography. *J. Geophys. Res.* **82,** 3842–3859 (1977).
2. Ladant, J., Donnadieu, Y., Lefebvre, V. & Dumas, C. The respective role of atmospheric carbon dioxide and orbital parameters on ice sheet evolution at the Eocene–Oligocene transition. *Paleoceanography* **29,** 1–14 (2014).
3. Pearson, P. N., Foster, G. L. & Wade, B. S. Atmospheric carbon dioxide through the Eocene–Oligocene transition. *Nature* **461,** 1110–1113 (2009).
4. Eagles, G., Livermore, R. & Morris, P. Small basins in the Scotia Sea: the Eocene Drake passage gateway. *Earth Planet. Sci. Lett.* **242,** 343–353 (2006).
5. Pagani, M. *et al*. The role of carbon dioxide during the onset of Antarctic glaciation. *Science* **334,** 1261–1264 (2011).
6. Sijp, W. P. *et al*. The role of ocean gateways on cooling climate on long timescales. *Glob. Planet. Change* **119,** 1–22 (2014).
7. Yang, S., Galbraith, E. & Palter, J. Coupled climate impacts of the Drake Passage and the Panama Seaway. *Clim. Dynam.* **43,** 37–52 (2013).
8. Borrelli, C., Cramer, B. S. & Katz, M. E. Bipolar Atlantic deepwater circulation in the middle-late Eocene: effects of Southern Ocean gateway openings. *Paleoceanography* **29,** 308–327 (2014).
9. Abelson, M., Agnon, A. & Almogi-Labin, A. Indications for control of the Iceland plume on the 'greenhouse-icehouse' climate transition. *Earth Planet. Sci. Lett.* **265,** 33–48 (2008).
10. Hodell, D. A., Venz, K. A., Charles, C. D. & Ninneman, U. S. Pleistocene vertical carbon isotope and carbonate gradients in the South Atlantic sector of the Southern Ocean. *Geochem. Geophys. Geosyst.* **4,** 1–19 (2003).
11. Langton, S. J., Rabideaux, N. M., Borrelli, C. & Katz, M. E. Southeastern Atlantic deep-water evolution during the late-middle Eocene to earliest Oligocene (Ocean Drilling Program Site 1263 and Deep Sea Drilling Project Site 366). *Geosphere* **12,** 1032–1047 (2016).
12. Zanazzi, A., Kohn, M., MacFadden, B. J. & Terry, D. O. Jr Large temperature drop across the Eocene–Oligocene transition in central North America. *Nature* **445,** 639–642 (2007).
13. Hren, M. T. *et al*. Terrestrial cooling in Northern Europe during the Eocene–Oligocene transition. *Proc. Natl Acad. Sci. USA* **110,** 7562–7567 (2013).
14. DeConto, R. M. & Pollard, D. Rapid Cenozoic glaciation of Antarctica induced by declining atmospheric CO_2. *Nature* **421,** 245–249 (2003).
15. Walker, J. C. G., Hays, P. B. & Kasting, J. F. A negative feedback mechanism for the long-term stabilization of Earth's surface temperature. *J. Geophys. Res.* **86,** 9776–9782 (1981).
16. Zeebe, R. E. & Caldeira, K. Close mass balance of long-term carbon fluxes from ice-core CO_2 and ocean chemistry record. *Nat. Geosci.* **1,** 312–315 (2008).
17. Berner, R. A., Lasaga, A. C. & Garrels, R. M. The carbonate-silicate geochemical cycle and its effect on atmospheric carbon dioxide over the past 100 million years. *Am. J. Sci.* **283,** 641–683 (1983).
18. Goddéris, Y., Donnadieu, Y., Le Hir, G., Lefebvre, V. & Nardin, E. The role of palaeogeography in the Phanerozoic history of atmospheric CO_2 and climate. *Earth-Sci. Rev.* **128,** 122–138 (2014).
19. Maher, K. & Chamberlain, C. P. Hydrologic regulation of chemical weathering and the geologic carbon cycle. *Science* **343,** 1502–1504 (2014).
20. Dessert, C., Duprè, B., Gaillardet, J., François, L. M. & Allègre, C. J. Basalt weathering laws and impact of basalt weathering on the global carbon cycle. *Chem. Geol.* **202,** 257–273 (2003).
21. Dalai, T. K., Ravizza, G. E. & Peucker-Ehrenbrink, B. The Late Eocene $^{187}Os/^{188}Os$ excursion: chemostratigraphy, cosmic dust flux and the Early Oligocene glaciation. *Earth Planet. Sci. Lett.* **241,** 477–492 (2006).
22. Goldner, A., Herold, N. & Huber, M. Antarctic glaciation caused ocean circulation changes at the Eocene–Oligocene transition. *Nature* **454,** 979–982 (2008).
23. Merico, A., Tyrrell, T. & Wilson, P. A. Eocene/Oligocene ocean de-acidification linked to Antarctic glaciation by sea-level fall. *Nature* **454,** 979–982 (2008).
24. Diester-Haass, L. & Zahn, R. Eocene–Oligocene transition in the Southern Ocean: history of water mass circulation and biological productivity. *Geology* **24,** 163–166 (1996).
25. Pusz, A. E., Thunell, R. C. & Miller, K. G. Deep water temperature, carbonate ion, and ice volume changes across the Eocene–Oligocene transition. *Paleoceanography* **26** (2011).
26. Cramer, B. S., Toggweiler, J. R., Wright, J. D., Katz, M. E. & Miller, K. G. Ocean overturning since the Late Cretaceous: inferences from a new benthic foraminiferal isotope compilation. *Paleoceanography* **24** (2009).
27. Coxall, H. K., Wilson, P. A., Pälike, H., Lear, C. H. & Backman, J. Rapid stepwise onset of Antarctic glaciation and deeper calcite compensation in the Pacific Ocean. *Nature* **433,** 53–57 (2005).
28. Liu, Z. *et al*. Global cooling during the Eocene–Oligocene climate transition. *Science* **323,** 1187–1190 (2009).
29. Plancq, J., Mattioli, E., Pittet, B., Simon, L. & Grossi, V. Productivity and sea-surface temperature changes recorded during the late Eocene-early Oligocene at DSDP Site 511 (South Atlantic). *Palaeogeogr. Palaeoclimatol. Palaeoecol.* **407,** 34–44 (2014).

Acknowledgements

We thank J. Higgins for insightful discussions, and for inspiring us to consider the role of silicate weathering. Computational resources were provided by the Canadian Foundation for Innovation (CFI) and Compute Canada, through a resource allocation to E.G. Simulations were integrated on the Scinet general purpose cluster at the University of Toronto. The Canadian Institute for Advanced Research (CIFAR) and the Spanish Ministry of Economy and Competitiveness, through the María de Maeztu Programme for Units of Excellence in R&D (MDM-2015-0552), supported involvement of E.G. and an NSERC Discovery grant supported involvement of G.H.

Author contributions

G.E. compiled geochemical data and prepared the manuscript. E.G. prepared the manuscript, performed model simulations and analysed simulation results. G.H. prepared the manuscript and assisted in analysis of geochemical data. S.Y. performed the model simulations and analysed simulation results.

Additional information

Supplementary information is available in the online version of the paper. Reprints and permissions information is available online at www.nature.com/reprints. Correspondence and requests for materials should be addressed to G.E.

Competing financial interests

The authors declare no competing financial interests.

Methods

The physical model. The model used in this study is CM2Mc[30], a three-degree version of NOAA GFDL's coupled climate model. The ocean circulation model is coupled to a fully dynamic three-dimensional atmosphere (AM2) and the GFDL thermodynamic–dynamic sea ice model (SIS). The model does not apply any flux adjustments, enabling it to simulate atmosphere/ocean–sea-ice feedbacks including salinity and temperature feedbacks in the ocean. The circulation is very similar to that of the GFDL ESM2M model, which is generally highly ranked among comprehensive coupled climate models.

Simulations. To investigate the impact of the Drake Passage deepening on ocean circulation and global climate, two simulations were performed with the Drake Passage sill depth set to 300 m and 1,500 m. The Panama Seaway is opened in both experiments by changing four land cells to 2,000-m-deep ocean cells. Otherwise, the standard modern topography and continental positions were used. Although there were many other notable differences in geography between the Eocene and today, uncertainty in the tectonic reconstructions and the inability of the relatively coarse-resolution model to simulate fine-scale circulation features could lead to incorrect artefacts in the simulated circulations; by starting from a well-vetted ocean bathymetry, we can provide a more confident estimation of the impact of Drake Passage opening. Atmospheric p_{CO_2}, orbital configuration, land cover and ice sheet extent are kept at pre-industrial levels. Each simulation was integrated for 1,400 years with the analysis being made on the last 100 years. See ref. 7 for more details on the simulations.

To estimate how precipitation over land would have changed as a function of CO_2, a suite of simulations was carried out using modern ocean bathymetry, with specified atmospheric CO_2 concentrations. For each CO_2 concentration, four simulations were carried out, two of which used a low value of obliquity for Earth's rotational axis (22°) and two of which used high obliquity (24.5°). For each value of obliquity, two precessional phases were used, to simulate intense boreal seasons and intense austral seasons. All simulations were integrated for at least 1,200 years. This suite of simulations allows the impact of CO_2 on precipitation to be averaged across the relatively high-frequency changes in Earth's orbit, given that the long-term averages are relevant for the silicate weathering timescale.

Code availability. The model CM2Mc is available as one configuration of the public release of MOM5 (mom-ocean.org). The runscripts and output files are available from eric.d.galbraith@gmail.com on request.

Data availability. The authors declare that the data supporting the findings of this study are available within the article and its Supplementary Information files.

References

30. Galbraith, E. D. *et al*. Climate variability and radiocarbon in the CM2Mc earth system model. *J. Clim.* **24,** 4230–4254 (2011).

nature geoscience
SUPPLEMENTARY INFORMATION
DOI: 10.1038/NGEO2888

Enhanced weathering and CO_2 drawdown caused by latest Eocene strengthening of the Atlantic meridional overturning circulation

Geneviève Elsworth*, Eric Galbraith, Galen Halverson, Simon Yang

*To whom correspondence should be addressed: genevieve.elsworth@gmail.com

Spatial heterogeneity of weathering rates

An important consideration is the spatial heterogeneity in weathering rates, which span more than an order of magnitude over the Earth surface. Variations in weathering rate are caused by differences in lithology and ground cover[1,2], as well as changes in precipitation and temperature[3]. Given that fully predictive models for weathering rates are still under development[4], we do not attempt to explicitly calculate weathering rates, but instead qualitatively consider how spatial heterogeneity would be expected to have influenced the net impact of the simulated AMOC-driven changes in temperature and precipitation on global silicate weathering. We do so by first comparing the simulated temperature and precipitation changes with the present-day distribution of weathering hotspots, and then consider whether or not continental drift would have altered the positions of these hotspots significantly since the latest Eocene.

Figures S2b and S2c show the simulated changes in temperature and precipitation in all regions with chemical weathering rates greater than 10 t km^{-2} a^{-1}, as calculated ignoring soil shielding (the distribution of these high-weathering rate regions is similar when soil shielding is considered, regardless)[4]. The model simulates a 0 to >30% increase in precipitation in most of these regions when the AMOC is established by Drake Passage deepening; only southeastern Africa shows a significant decrease in precipitation. In addition, most of these regions show a positive temperature change; a large part of northern South America experiences a mild cooling, but this effect on weathering rates would have been offset by the large increase in precipitation.

The model simulates significantly enhanced precipitation in the circum-North Atlantic, including Greenland and Western Europe. In the late Eocene, these regions, along with significant areas of now-submerged continental crust (e.g. the Rockall Plateau and the continental margins adjacent to Greenland and western Europe), would have been more prone to chemical weathering due to widespread mantling of relatively fresh basalt of the North Atlantic Igneous Province[5] and more pronounced topography due to uplift on the flanks of the growing North Atlantic Ocean. Meanwhile, a smaller increase in precipitation and a negligible temperature change in the present-day weathering hotspot of southeast Asia suggest a small, but nonetheless positive change of weathering rates in this important region. Hence, consideration of the spatial distribution of modern weathering hotspots confirms the expectation that prior to the Eocene-Oligocene boundary, AMOC establishment would have led to an overall increase in chemical weathering and a commensurate decrease in atmospheric pCO_2.

Figure S3 shows a tectonic reconstruction for the latest Eocene. Comparison with Figure S2 shows that most of the weathering hotspots were located in nearly the same positions as today relative to the equator. Because the AMOC-driven changes are dominated by changes in the large-scale Hadley circulation, analogous to the "bipolar see-saw" changes of the Quaternary[6,7,8], small longitudinal changes in continental positions are unlikely to have greatly impacted the distribution of AMOC-induced precipitation and temperature changes. The most important tectonic changes have occurred around the Indian Ocean. The reconstruction suggests that the Indian plate was located further south than today (but still north of the equator) while Western Indonesia was located further north and eastern Indonesia was located further south. The distribution of a majority of these important regions north of the equator would imply a likely overall increase in precipitation and temperature under the late Eocene configuration, just as simulated in the model, though it may have been a smaller increase in these regions than simulated with the modern plate positions. An important caveat is that the western Pacific warm pool and Indian Ocean circulation would have been significantly different at this time, a contrast that could have modified the local response to the AMOC change. This contrast would benefit from further study.

Osmium isotope record

Osmium isotope ratios ($^{187}Os/^{188}Os$) in marine sediments are sensitive to changes in continental silicate weathering rates due to the low residence time of Os in the oceans (~1-5 x 10^4 years) and the strong isotopic contrast between average continental ($^{187}Os/^{188}Os \approx 1.4$) and unradiogenic (typically mafic) igneous ($^{187}Os/^{188}Os \approx 0.13$) sources[9]. Os isotopes also record large impact events as short-duration anomalies because extraterrestrial material is rich in Os compared to the continental crust and unradiogenic igneous sources. For example, declining Os isotope ratios in the late Maastrichtian clearly show the influence of weathering the Deccan Traps in the 0.5 m.y. leading up the Cretaceous-Paleogene boundary, punctuated by an excursion at the boundary itself, corresponding to the Chicxulub impact[10].

The Cenozoic seawater $^{187}Os/^{188}Os$ record shows broadly increasing values, likely reflecting the decreased weathering of large igneous provinces (LIPs) associated with the opening of the southern and central Atlantic Ocean and the influence of Alpine-Himalayan orogenesis. This trend is interrupted in the late Eocene by a large anomaly, where a decline in $^{187}Os/^{188}Os$ from ~0.52 to 0.3 and subsequent recovery closely corresponds with the proposed ca. 1.5 m.y. interval of strong AMOC preceding onset of Antarctic glaciation (Fig. 1d in the main manuscript). This pattern is a positive test of the hypothesis that the transiently strong AMOC in the late Eocene resulted in intensified weathering of mafic terranes, which would have efficiently drawn down atmospheric $p\mathrm{CO_2}$ due to their high weatherability. While we cannot unambiguously identify which mafic terranes were responsible for this unradiogenic Os influx, the relatively recent (ca. 60 Ma) North Atlantic Volcanic Province (NAVP) was a likely contributor. These mafic volcanics, which include abundant picrite and other Mg-rich basalts[11,12], were extruded subaerially over a large area of the North Atlantic, spanning form Baffin Island and southern Greenland across the Rockall Plateau to the margin of western Europe – a region that experienced some of the most extreme increases in temperature and precipitation in the AMOC simulation (Fig. S2a and S2c).

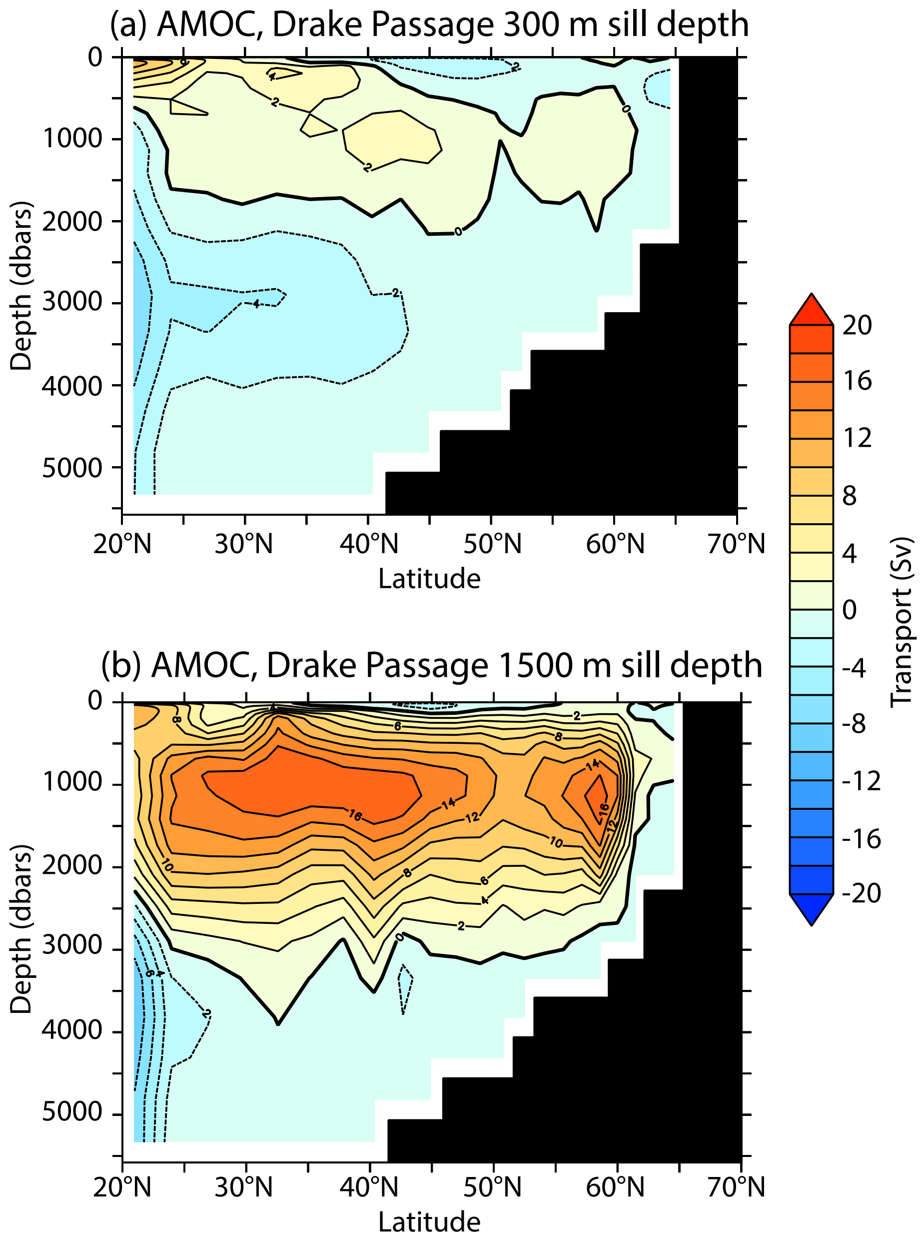

Figure S1: Simulated impact of Drake Passage deepening on strength of the Atlantic Meridional Overturning Circulation (AMOC) measured in Sverdrups (Sv, 10^6 m^3 s^{-1}). (a) Simulated AMOC strength at a Drake Passage sill depth of 300 m. (b) Simulated AMOC strength at a Drake Passage sill depth of 1500 m.

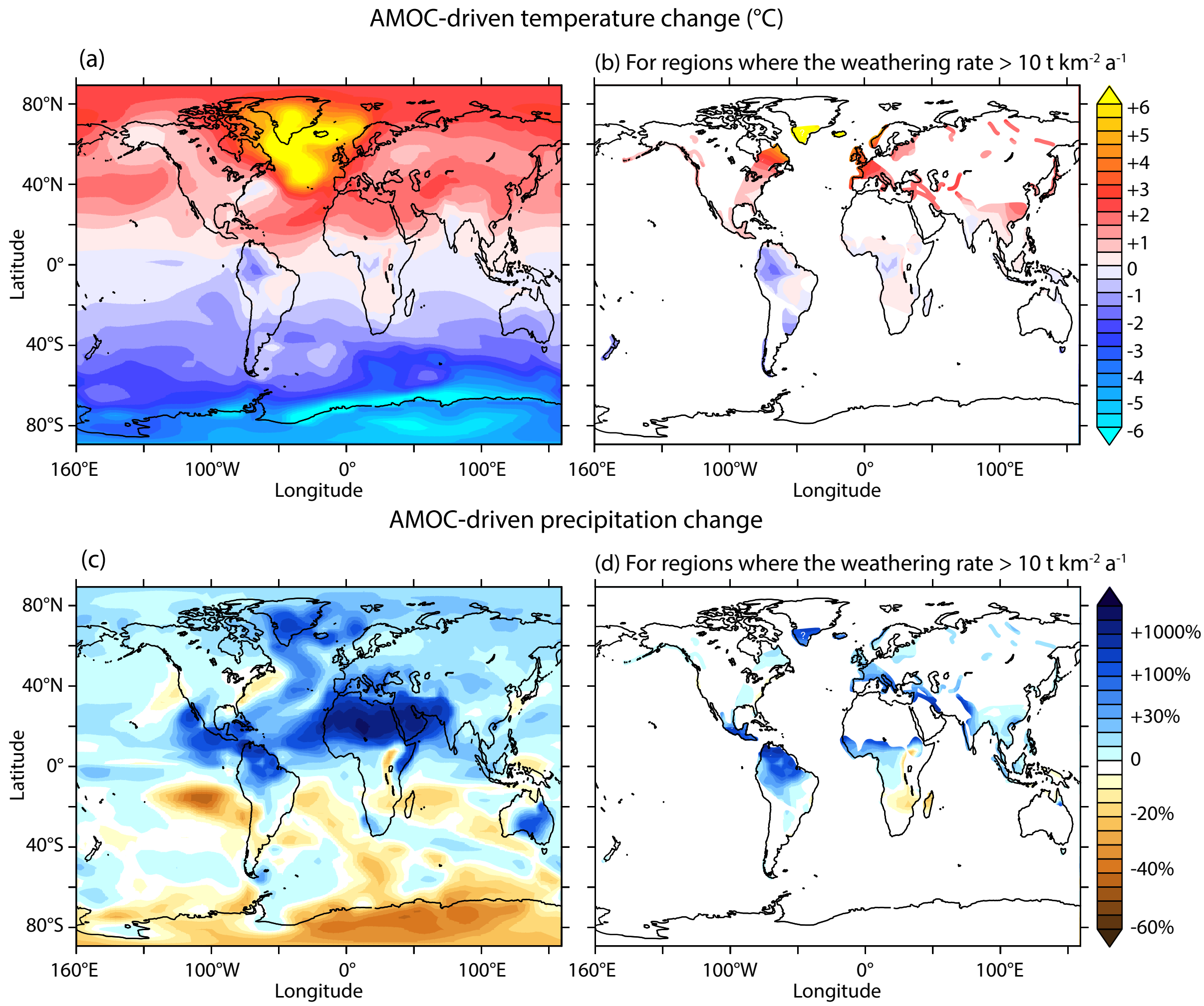

Figure S2: Simulated distribution of the AMOC-driven changes in temperature and precipitation in the CM2Mc model in regions with high chemical weathering rates. (a) Simulated changes in temperature resulting from the deepening of the Drake Passage sill depth from 300m to 1500m. (b) Same as (a) but shown only for regions with chemical weathering rates greater than 10 t km^{-2} a^{-1} as calculated by Hartmann et al. (2014). (c) Simulated changes in precipitation resulting from the deepening of the Drake Passage sill depth from 300 to 1500 m (d) Same as (c) but shown only for regions with chemical weathering rates greater than 10 t km^{-2} a^{-1} as calculated by Hartmann et al. (2014).

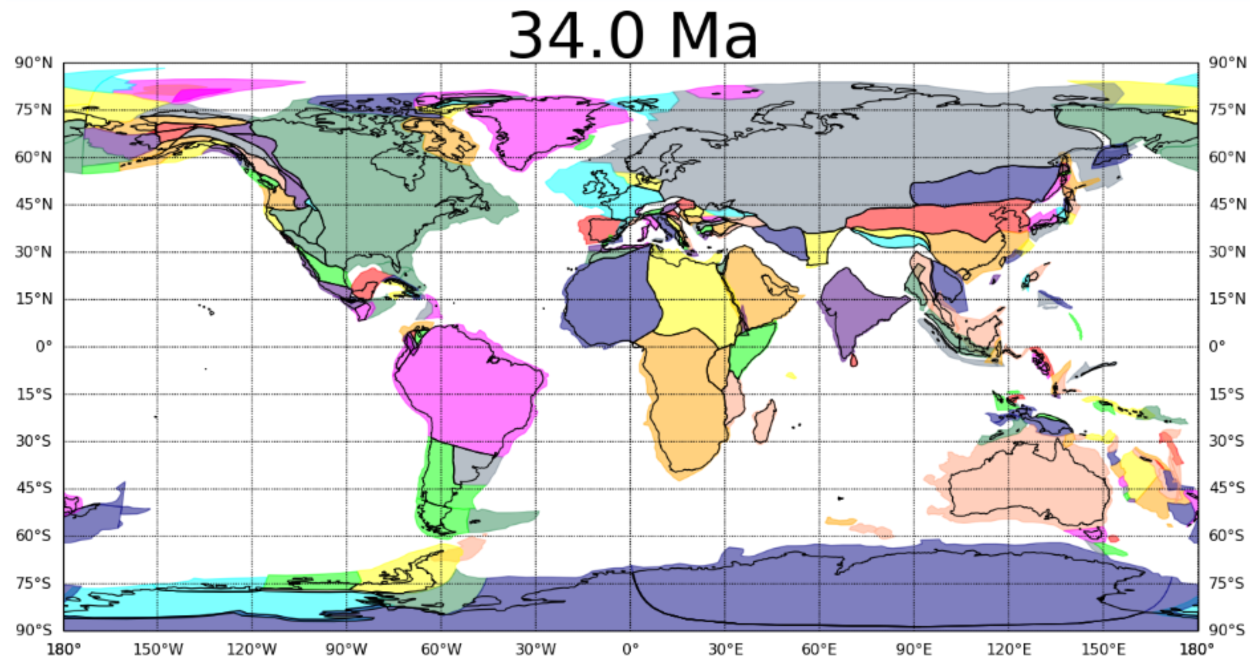

Figure S3: Plate tectonic reconstruction for latest Eocene (34.0 Ma) using the default model of GPlates (http://portal.gplates.org/map/). Note the more southerly positions of India and eastern Indonesia, which may have led to a smaller increase in precipitation in these regions than simulated by the model.

References:

1. West, J. A., Galy, A. & Bickle, M. Tectonic and climatic controls on silicate weathering. *Earth Planet. Sci. Lett.* **235**, 211-238 (2005).

2. Goddéris, Y., Roelandt, C., Schott, J., Pierret, M. & François, L. M. Towards an Integrated Model of Weathering, Climate, and Biospheric Processes. *Rev. Mineralogy & Geochemistry*. **70**, 411-434 (2009).

3. Kump, L. R., Brantley, S. L. & Arthur, M. A. Chemical Weathering, Atmospheric CO_2, and Climate. *Ann. Rev. Earth Planet Sci.* **28**, 611-667 (2000).

4. Hartmann, J., Moosdorf, N., Lauerwald, R., Hinderer, M. & West, A. J. Global chemical weathering and associated P-release – The role of lithology, temperature and soil properties. *Chem. Geol.* **363**, 145-163 (2014).

5. ^{40}Ar-^{39}Ar Ages of Lavas from the Southeast Greenland Margin, ODP Leg 152, and the Rockall Plateau, DSDP Leg 81. *Proc. Ocean Drilling Program, Scientific Results*. **152**, 387-402 (1998).

6. Wang, Y. J., Cheng, H., Edwards, R. L., An, Z. S., Wu, J. Y., Shen, C. C. & Dorale, J. A. Absolute-Dated Late Pleistocene Monsoon Record from Hulu Cave, China. *Science*. **294**, 2345-2348 (2001).

7. Broccoli, A. J., Dahl, K. A. & Stouffer, R. J. Response of the ITCZ to Northern Hemisphere cooling. *Geophys. Res. Lett.* **33**, (2006).

8. Brown, N. & Galbraith E. D. Hosed vs. unhosed: interruptions of the Atlantic Meridional Overturning Circulation in a global coupled model, with and without freshwater forcing. *Clim. Past*. **12**, 1663-1679 (2016).

9. Peucker-Ehrenbrink, B. & Ravizza, G. Osmium isotope stratigraphy. *The Geologic Time Scal3 2012*. 145-166 (2012).

10. Ravizza, G. & Peucker-Ehrenbrink, B. Chemostratigraphic Evidence of Deccan Volcanism from the Marine Osmium Isotope Record. *Science*. **302**, 1392-1395 (2003).

11. Graham, D. W., Larsen, L. M. Hanan, B. B., Storey, M. Pedersen, A.K. & Lupton, J. E. Helium isotope composition of the early Iceland mantle plume inferred from the Tertiary picrites of West Greenland. *Earth Planet. Sci. Lett*. **160**, 241-255 (1998).

12. Stuart, F. M., Lass-Evans, S., Fitton, J. G. & Eliam, R. M. High $^{3}He/^{4}He$ ratios in picritic basalts from Baffin Island and the role of a mixed reservoir in mantle plumes. *Nature*. **424**, 57-59 (2003).